RSC Advances

This article can be cited before page numbers have been issued, to do this please use: X. Li, F. Qi, Y. Xue, C. Yu, H. Jia, Y. Bai, S. Wang, Z. Liu, J. Zhang and C. Tang, *RSC Adv.*, 2016, DOI: 10.1039/C6RA20671A.

Porous boron nitride coupled with CdS for adsorption-photocatalytic synergistic removal of RhB†

Xiaopeng Li[a], Feng Qi[a], Yanming Xue[b], Chao Yu[a], Huichao Jia[a], Yinghao Bai[a], Sai Wang[a], Zhenya Liu[a], Jun Zhang*[a] and Chengchun Tang*[a]

[a]School of Material Science and Engineering and Hebei Key Laboratory of Boron Nitride Micro and Nano Materials, Hebei University of Technology, Tianjin 300130, P. R. China

[b]World Premier International Center for Materials Nanoarchitectonics (WPI-MANA), National Institute for Materials Science (NIMS), Namiki 1-1, Tsukuba, Ibaraki 305-0044, Japan

*Corresponding author. Tel.: +86-22-60202660; fax: +86-22-60202660

E-mail address: junnano@gmail.com (J. Zhang), tangcc@hebut.edu.cn (C. Tang).

† *Electronic Supplementary Information (ESI) available: [details of any supplementary information available should be included here]. See DOI: 10.1039/x0xx00000x*

Abstract: Porous boron nitride (a-BN) modified by uniformly dispersed CdS photocatalysts were successfully prepared using the facile hydrothermal method, and probed by electron microscopy, X-ray diffraction and Uv-vis diffuse reflection spectra. Adsorption and photocatalytic activities were evaluated using high concentration Rhodamine B (RhB) as a target organic pollutant. The results show that after adding a small amount of CdS nanoparticles, the absorbent can self-regenerate with the assistant of visible light irradiation to photocatalytically degrade the organic pollutants adsorbed on the surface of a-BN/CdS. During the adsorption and photocatalytic process, boron nitride could supply a concentrated pollutant environment around CdS photocatalyst active sites. The optimal loading amount of CdS was observed to be 0.5 wt% with the best adsorption-photocatalytic synertistic efficiency, which was probably due to the better dispersion of CdS on a-BN support and the separation of photogenerated electron-hole pairs by negatively charged a-BN. The photocatalytic mechanism of the a-BN/CdS composite was also investigated by radical trapping experiments.

View Article Online
DOI: 10.1039/C6RA20671A

1. Introduction

Recently, industrialization and agricultural development, together with rapid urbanization, have caused serious environmental pollution especially on water resources.[1, 2] Various kinds of contaminants enter into water sources through industrial wastewater discharge. Among them, organic dyes generated from dyestuffs, textile, paper, cosmetics, plastics, and paint industries are considered as the primary pollutants in wastewater. Most dyes, even at very low concentrations in water, are pose serious hazard to human and aquatic ecosystems. As a result, effective removal of organic pollutants from wastewater becomes an important issue to many researchers and governments taking advantage of new materials and techniques. Among the various approaches available for the removal of dyestuffs, adsorption by using absorbent materials, including activated carbon, natural materials and bioabsorbent, has been considered to be the most common and promising process as compared to other traditional treatment methods due to its low-cost, easy availability, and high efficiency.[3-6] It has been demonstrated that recently developed BN materials with porous structure can be considered as one of the most promising absorbent for the removal of dyes from water due to their high specific surface area, numerous density defects, high stability under harsh conditions, and high resistance to oxidation.[7-11] Great progresses have been made to improve adsorption performance based on porous BN by our group.[12, 13]

However, it should be noted that the adsorption technique merely transfers organic compounds from water to absorbents thus creates secondary pollution, and the absorbents can be easily inactive after saturation adsorption. In addition, the regeneration of the absorbent costs more to the process, and the adsorption efficiency after regeneration is generally reduced. It is highly important to find out an effective way to remove dye after adsorption while without secondary pollution and regeneration process. As known, the use of photocatalysis has been proven to be an effective chemical method for the destruction and removal of dyes under light irradiation.[14] For the purpose of overcoming the drawbacks of adsorption, combining absorbent with photocatalysts is considered as an effective and potential method for

the treatment of dyes from wastewater by means of the so-called synergistic effect. This strategy has been widely adopted in silica, activated carbon, and zeolite absorbent for the degradation of dye-containing wastewater.[15-17] To the best of our knowledge, the synergistic effect has seldom been investigated in porous BN focusing on their excellent adsorption performance with assistive photocatalysts. This is because our attentions are mainly drawn on the excellent photocatalysis performance just introducing low proportional BN materials as immobile support.[18-23]

Given the excellent cationic dye adsorption performance of porous BN and visible-light-driven photocatalytic property of CdS (Band gap ~2.4 eV)[13, 24-26], it is of interest to see whether one can develop a BN-CdS heterostructure by coupling CdS to porous BN absorbent, which can provide synergies for achieving better dye removal performance in wastewater. The synthesis and characterization of BN-CdS heterostructure and its adsorption-photocatalytic activity in aqueous solution using Rhodamine B (RhB) dye as a model contaminant are discussed.

2. Experimental

2.1 Preparation of porous boron nitride (a-BN)

The porous BN fibers were prepared according to our reported method.[27] Typically, 3.71 g of boric acid and 3.78 g of melamine at a molar ratio of 1:2 were dissolved into 300 ml of distilled water. The reaction mixtures were heated at 90 ℃ for 12 h, and then naturally cooled to room temperature to get a white precipitate ($C_3N_6H_6 \cdot 2H_3BO_3$, namely, M·2B). Finally, uniform-morphology a-BN fibers were formed via a pyrolytic process of M·2B at 1050 ℃ for 4 h in a flow of N_2.

2.2 Synthesis of a-BN/CdS hybrid materials

The a-BN/CdS composites were synthesized by a simple hydrothermal method. For the sake of convenience, the obtained composites were labeled as x % a-BN/CdS, in which x denotes wt% of CdS compared with a-BN in a-BN/CdS. The typical synthesis of the 0.5 % a-BN/CdS materials was as follows: 0. 5 g of a-BN as the substrate was added into 80 ml of distilled water and stirred magnetically for 12 h.

Then, 5.34 mg of cadmium nitrate tetrahydrate ($Cd(NO_3)_2 \cdot 4H_2O$) was added into the above suspension and stirred for 3 h. Further, a stoichiometric amount of thiourea was added and further stirred for 30 min. After sonication for 30 min, the mixture was transferred into a Teflon-lined stainless steel autoclave and kept at 100 ℃ for 2 h in an electric oven. After cooling down to room temperature naturally, the light yellow product was washed with distilled water and absolute ethanol for several times, and dried at 60 ℃ for 24 h for further test. Similarly, the 0.3 % and 1 % composites were also obtained. The bulk CdS was synthesized by the same method just without addition of a-BN

2.3 Characterization

The structure and morphology of the samples were examined using X-ray powder diffraction (XRD, BRUKER D8 FOCUS) and field emission scanning electron microscopy (SEM, HITACHI S-4800). Transmission electron microscopy (TEM) micrographs were taken with a Tecnai F20 electron microscope (Philips, Netherlands) with an acceleration voltage of 200 kV. Ultraviolet–visible (UV–vis) diffuse reflection spectra (DRS) were collected at room temperature with a UV–vis spectrophotometer (HITACHI, U-3900H) in the range of 200-800 nm and $BaSO_4$ was used as the reflectance standard material. Photoluminescence spectra (PL) of the samples were recorded on a HITACHI F-7000 fluorescence spectrophotometer. The concentration of the cadmium ion was measured by an inductively coupled plasma emission spectroscopy (TELEDYNE-Leeman Labs, USA).

2.4 Adsorption and photocatalytic degradation experiments

The batch equilibrium experiment was typically carried out to study the adsorption behavior by adding a fixed amount of a-BN/CdS powders (0.1 g) into 160 ml of RhB aqueous solution with an initial concentration of 100 mg L^{-1}. The dispersion was stirred in dark for 6 h to favor the adsorption/desorption equilibrium. During the period, about 5 ml of the suspension sample was collected at particular time intervals, then immediately centrifuged and filtered to remove the particles and

View Article Online
DOI: 10.1039/C6RA20671A

subjected to UV-vis analysis.

In order to prove that a-BN/CdS was a dual functional composite with adsorptive and visible-light-driven photocatalytic capabilities; the above mixture after adsorption equilibrium was exposed to the visible-light irradiation under magnetic stirring to regenerate the powder. A 300 W Xe light (CEL-HXUV300, Zhongjiao Aulight Science & Technology Co. Ltd., Beijing, China) with a 420 nm cutoff filter was used as the visible-light source. The reaction system was cooled by circulating water and maintained at room temperature. At the same time, aeration was performed using an air pump to ensure a constant supply of oxygen and to complete mixing of the solution and the powder during photoreactions. During irradiation, ~5 ml of the suspension continually was taken from the reaction cell at given time intervals and centrifuged to remove the particles.

To obtain the adsorptive and photocatalytic degradation removal ratio of RhB on the a-BN/CdS composites, the RhB concentration was analyzed by UV-vis spectrophotometer at a wavelength of 553 nm. A complete cycle was composed of adsorption and photocatalysis steps described above. The total removal rate of RhB was contributed by both the adsorptive and photocatalytic process.

3. Results and discussion

3.1 Characterization of prepared samples

The crystallographic structure and phase composition of a-BN, a-BN/CdS and bulk CdS are displayed in Fig. 1. As can be seen, the diffraction peaks at ~25.5 ° and ~42.6 ° can be indexed to the (002) and (100) crystal planes of BN (JCPDS No. 34-0421). The porous BN with a turbostratic structure can be judged from the two peaks being broaden, which has been often observed in our previous reports.[12] The pattern for pure bulk CdS matches well with the standard spectra (JSPDS No. 1-783) with the prominent diffraction peaks corresponding to (100), (002), (101), (102), (110), (103) and (112), which indicates that CdS particles could be obtained in such reaction condition with $Cd(NO_3)_2 \cdot 4H_2O$ and thiourea. After coupling CdS to a-BN, in

these patterns of a-BN/CdS with different CdS loading, peaks corresponding to BN are clearly detected, but that of CdS in the composites has hardly been found. This may be due to the low amount of CdS in the composites, the enough small CdS particles and the good dispersion of CdS on a-BN support. We speculate that CdS particles should be formed despite small amount in the composites, judging from samples looked yellow from the color of CdS as shown by the optical pictures in the inset of Fig. 1. It is clear to see that three a-BN/CdS samples exhibit similar XRD patters, in which the peak corresponding to (002) is sharper than that of pure BN. The sharper peak indicates the good crystallinity after coupling with CdS, which could be attributed to the fact the improved crystallinity after hydrothermal treatment for a-BN in high temperature and pressure condition. Also, the superposition of the diffraction peak between the (002) plane of the CdS and the (002) plane of the BN may also contribute to this result. Besides, no other diffraction peaks could be observed in the patters of composites, indicating that the introduction of CdS did not cause the development of new crystal orientations.

In order to investigate the morphology, study the role of a-BN and analyze the effect of the CdS particles on the microscopic structure of the a-BN/CdS composites, SEM and TEM analysis were performed. In the SEM analysis (Fig. 2a and Fig. S1-a), it could be found that the pure porous BN with white color has a ribbon-like microscopic structure and relatively smooth surface, which is consistent with our previous results.[12] SEM micrographs of samples, which contain different CdS content (0.3 %, 0.5 % and 1 %), are shown in Fig. 2b, c, and d, respectively. It could be seen that CdS particles are all uniformly distributed on the surface of a-BN, no apparent agglomeration of CdS in local area is discerned in 0.3 % and 0.5 % a-BN/CdS samples, demonstrating that the microstructure of a-BN is beneficial to the dispersion of CdS. Amount of CdS nanoparticles on porous BN surface augments with increasing of CdS content in composites. In both of the two composites, the particles size is almost the same, from 60 to 80 nm (Fig. S1-b). However, when 1 % CdS was loaded, the as-formed CdS particles are inclined to agglomerate (Fig. 2d). It suggests

that the CdS particles are easier to agglomerate on the surface of a-BN support with increasing the loading amount. Compared with the 0.3 % and 0.5 % a-BN/CdS composites with homogeneously deposited of CdS, the agglomerated CdS particles in the 1 % a-BN/CdS sample may hamper the dye adsorption and light incidence on these photoreactive sites and consequently reduce its dye remove efficiency. From the serious decrease of special surface area of a-BN/CdS compared with pure BN (Fig. S2), we speculate that the CdS particles deposited not only on the surface but also on the pores of porous BN due to the in-situ formation process of heterostructure.

The morphology of the 0.5 % a-BN/CdS composite was further analyzed by TEM (Fig. 3). It is clear to see that a small amount of CdS nanoparticles (black region) with deep contrast are dispersed onto the surface of porous BN, and a heterojunction structure might be formed in Fig. 3a. From this image, we can also observe the representative porous BN ribbon possessing porous, rippled, and corrugated structure.[12] In order to confirm the heterostructure between the a-BN and CdS nanoparticles, it has also been investigated by HRTEM in Fig. 3b. These reflect the good interfacial contact between a-BN and CdS nanoparticles. About 0.35 nm crystal lattice interspacing corresponding to a-BN substrate was figured out, which is characteristic of d_{0002} spacing in the turbostratic BN materials. In addition, it can be seen clearly that the CdS nanoparticles with high degree of crystallinity were grown on the edge of a-BN, which is consistent with the SEM observation. The distinct crystalline interplanar spacing was figured out as 0.336 nm, which can be ascribed to the (002) crystallographic plane of CdS. The perfect lattice match between a-BN and CdS endow the close contact each other, which is highly expected to improve the separation of photo-induced electrons and holes.

Considering that the optical absorption properties play an important role in affecting the photocatalytic activity of semiconductors, the UV-vis diffuse reflection spectra of a-BN, a-BN/CdS, and bulk CdS were investigated and results are given in Fig. 4. It could be seen that a-BN exhibits the adsorption in the region ranging from 200 nm to 300 nm with a low visible light absorption. Meanwhile, the pure bulk CdS

presented strong absorption from the UV light to visible light shorter than approximately 580 nm. As for the a-BN/CdS composite samples, there are two sets of absorption bands, one is a shoulder at ~300 nm corresponding to a-BN, another is located at ~550 nm ascribing to the introduction of CdS nanoparticles. The coupling of CdS onto a-BN results a significant blue shifts of the absorption band with respect to the bare CdS. These shifts indicate that the band gap of the CdS nanoparticles widens owing to hybridization with the higher-band-gap BN materials,[22] in which the a-BN supports restrain the growth of CdS crystalline grain. With the increasing CdS contents in the a-BN/CdS composites, the samples' color gradually changes more yellow (inset in Fig. 1) and the visible light absorption ability of the composites is gradually enhanced. This enhancement would also have affected their photocatalytic activities. The results indicate that the as synthesized composites have suitable band gap for the photocatalytic decomposition of organic contaminants under visible light irradiation.

3.2 Adsorption and photocatalytic activity of photocatalysts

To evaluate the synergistic adsorption and photocatalytic acitivity of prepared absorbent/photocatalysts, the 0.3 % a-BN/CdS, 0.5 % a-BN/CdS, 1 % a-BN/CdS and bulk CdS samples were applied to remove RhB from water. The adopted RhB solution has an initial concentration of 100 mg/L, in which the concentration was too high to be used for normal semiconductor photocatalysts test, whereas it is suitable for adsorption performance evaluation for adsrobents with high surface area. The adsorption and photocatalytic degradation processes of RhB on four samples are shown in Fig. 5a. In the adsorption-desorption process (6 h duration) on these samples, it can be seen that the adsorption removal ratio of RhB over 0.3 % a-BN/CdS, 0.5 % a-BN/CdS, 1 % a-BN/CdS and bulk CdS are 35 %, 22 %, 15 % and 0.1 %, respectively. With the increase of the CdS loading, the amount of adsorbed RhB by the composites reduces, and yet still higher than that of the individual bulk CdS. The main reason may be ascribed to the reserved high surface area of porous BN after

View Article Online
DOI: 10.1039/C6RA20671A

coupling small amounts of CdS nanoparticles.

After adsorption-desorption equilibrium, photocatalytic reaction was performed under visible light illumination. From the blank test, we confirm that degradation without a photocatalyst does not occur, and the RhB molecule is stable under visble-light illumination. For 80 min duration, photocatalytic degradation removal ratios of RhB on 0.3 % a-BN/CdS, 0.5 % a-BN/CdS, 1 % a-BN/CdS and bulk CdS reach 55 %, 74 %, 33 % and 16.9 %, respectively. The photocatalytic degradation removal ratios over all of the three a-BN/CdS composite samples are higher than that of individual bulk CdS. The reason may be that RhB moleculres can be preferentially adsorbed onto a-BN from water and transferred to the active center of CdS in the composite to get a higher mass transfer speed. It means that a-BN can supply a concentrated dye environment to improve the photocatalytic efficiency of CdS. Among them, the 0.5 % a-BN/CdS composite exhibits the best photocatalytic degradation performance under visible-light illumination. That is to say, the more loading photocatalytic material of CdS in a-BN/CdS leads to the decreased photocatalytic activity, which may be due to the weakening of RhB adsorbed by a-BN with decreasing surface area. In all, the total removal ratios over four samples are 90 %, 96 %, 48 %, and 17 %, respectively. Therefore, the optimal loading CdS content is 0.5 %, in which the composite possesses the most excellent adsorption-photocatalytic synergistic efficiency.

Under visible light irradiation, the evolution of the adsorption spectra of RhB with reaction time for 0.5 % a-BN/CdS is shown in Fig. 5b. The max adsorption wavelength of RhB at 553 nm significantly decreased with increasing irradiation time, and the color of the RhB solution changed from red to light red and then disappeared. It has been observed that no new absorption peak appear in either the ultraviolet or visible region, which indicates that the chromophoric structure of the RhB dye was completely decomposed during the photocatalytic reaction.

View Article Online
DOI: 10.1039/C6RA20671A

3.3 Possible adsorption-photocatalytic synergistic mechanism

Radicals and holes trapping experiments were further conducted to evaluate the roles of primary reactive species during the irradiation of the 0.5 % a-BN/CdS sample. During the experiments, EDTA, isopropanol, and ascorbic acid were used as hole (h^+), hydroxyl ($^{\bullet}OH$), and superoxide ($^{\bullet}O_2^-$) radical scavengers, respectively. As shown in Fig. 6a, the addition of isopropanol had a little influence for photocatalytic activity, implying that hydroxyl radical was not the dominant active species. However, it was significantly suppressed when EDTA and ascorbic acid were introduced under the same conditions. The above results indicates that both h^+ and $^{\bullet}O_2^-$ radicals are the main active species in RhB photodegradation, and the superoxide plays the most important roles in this system.

Based on the above experimental results, the significant enhancement of dye removal ability for a-BN coupling with CdS could be attributed to the synergistic effect between a-BN and CdS. A possible adsorption-photocatalytic synergistic mechanism of a-BN/CdS is proposed in Fig. 6c. The porous BN provides plentiful adsorption sites to concentrate the RhB molecules diluted in aqueous solution. So the dye species are considered to be preferentially adsorbed on the surface of the a-BN support materials. By diffusion, the adsorbed dye molecules migrate to the CdS photocatalytical reaction centers. Under visible light irradiation, the transparent BN favors the light to transfer to the vicinity of CdS to form photo-generated electron-hole pairs, then further to generate various radicals to decompose dye pollutants. In addition, the CdS loaded on the absorbent of a-BN has less agglomeration compared to the individual bulk CdS, which is favorable to increase the photocatalytic actives. The presence of a-BN in photocatalyst system is also beneficial for passivating surface barrier; suppressing the recombination of photo-generated electron and holes.[18, 19, 28] The indirect evidence is given by the PL spectra of bulk CdS and 0.5 % a-BN/CdS samples recorded with an excitation wavelength of 325 nm in Fig. 6b. Bulk CdS shows a PL signal around 528 nm due to band-gap excitation, while the BN/CdS composite hardly shows any PL signal,

implying the electron or hole transfer from CdS to BN in BN/CdS photocatalysts thus with enhanced photocatalytic activity.

3.4 Stability evaluation

The high specific surface area, chemical durability and oxidation resistance render porous BN materials as an outstanding absorbent for pollutant adsorption.[9, 12] However, bare CdS suffers from an inherent drawback of photocorrosion, where S^{2-} in CdS is oxidized by photogenerated holes accompanied with leaching of toxic Cd^{2+}.[29, 30] The concentration of Cd^{2+} during the photocatalytic process was monitored by high dispersion inductively coupled plasma emission spectroscopy (ICP), as shown in Fig. 7a. For bulk CdS, with the increasing of illumination time, the concentration of Cd^{2+} gradually rises up to 186 ppm after 2 h. However, for the 0.5 % a-BN/CdS sample, the change of Cd^{2+} concentration is negligible. This result indicates that no evident photocorrosion occurs during the a-BN/CdS photocatalytic degradation process, in which the a-BN substrate can improve the photo-stability of CdS.

Considering the potential applications of a-BN/CdS composite for water treatment, the activity of the composite adsrobents/photocatalysts was further evaluated by recycle experiments using 0.5 % a-BN/CdS for the photocatalytic process under visible light irradiation. Fig. 7b shows the photocatalytic degradation of RhB for 5 runs of reactions after adsorption equilibrium for each time. The photocatalytic efficiency did not exhibit significant loss after five recycling runs. The slightly deactivation is due to the inevitable loss of photocatalysts during the recovery process. In addition, no distinct change of the corresponding XRD patterns of the 0.5 % a-BN/CdS composite before and after five times reuse was observed (Fig. S3). Therefore, we can say that the a-BN/CdS absorbent/photocatalyst is stable during photocatalytic process. This effect may be ascribed to the negatively charged BN surface, which could scavenge the photo-generated holes to prevent the photocorrosion in CdS.[20, 31]

View Article Online
DOI: 10.1039/C6RA20671A

4. Conclusions

The synthetic approach discussed here provides a facile way to uniformly disperse CdS nanoparticles over porous BN. The hybridization of CdS nanoparticles with a-BN fibers has led to a noticeable adsorption-photocatalytic synergetic activity for the decomposition of high concentration organic pollutants under visible light illumination. The photocatalytic performance of such composites is strongly dependent on its content of CdS. This work not only highlights the potential application of a-BN/CdS composites, but also provides useful information for adsorption-photocatalytic synergistic removal of pollutants on the hybridization of absorbents and photocatalysts. Currently, efforts are underway to utilize this strategy to explore another system of materials for synergistic removal of pollutants.

Acknowledgements

This work was supported by the National Natural Science Foundation of China (Grants No. 51372066, No.51332005 and No. 21103056), the Program for Changjiang Scholars and Innovative Research Team in University (PCSIRT: Grant No.IRT13060), and the Natural Science Foundation of Hebei Province (Grand No. B2016202213).

View Article Online
DOI: 10.1039/C6RA20671A

Notes and references

1. M. A. Shannon, P. W. Bohn, M. Elimelech, J. G. Georgiadis, B. J. Marinas and A. M. Mayes, *Nature*, 2008, **452**, 301-310.
2. M. A. Montgomery and M. Elimelech, *Environ. Sci. Technol.*, 2007, **41**, 17-24.
3. A. J. Brooks, L. Hyung-nam and E. K. James, *Nanotechnology*, 2012, **23**, 294008.
4. E. Forgacs, T. Cserháti and G. Oros, *Environ. Int.*, 2004, **30**, 953-971.
5. G. Crini, *Bioresour. Technol.*, 2006, **97**, 1061-1085.
6. X. Qu, J. Brame, Q. Li and P. J. J. Alvarez, *Acc. Chem. Res.*, 2013, **46**, 834-843.
7. P. Dai, Y. Xue, X. Wang, Q. Weng, C. Zhang, X. Jiang, D. Tang, X. Wang, N. Kawamoto, Y. Ide, M. Mitome, D. Golberg and Y. Bando, *Nanoscale*, 2015, **7**, 18992-18997.
8. W.-Q. Han, R. Brutchey, T. D. Tilley and A. Zettl, *Nano Lett.*, 2004, **4**, 173-176.
9. W. Lei, D. Portehault, D. Liu, S. Qin and Y. Chen, *Nat. Commun.*, 2013, **4**, 1777.
10. W. Meng, Y. Huang, Y. Fu, Z. Wang and C. Zhi, *J Mater. Chem. C*, 2014, **2**, 10049-10061.
11. Q. Weng, X. Wang, C. Zhi, Y. Bando and D. Golberg, *ACS Nano*, 2013, **7**, 1558-1565.
12. J. Li, X. Xiao, X. Xu, J. Lin, Y. Huang, Y. Xue, P. Jin, J. Zou and C. Tang, *Sci. Rep.*, 2013, **3**, 3208.
13. J. Li, Y. Huang, Z. Liu, J. Zhang, X. Liu, H. Luo, Y. Ma, X. Xu, Y. Lu, J. Lin, J. Zou and C. Tang, *J. Mater. Chem. A*, 2015, **3**, 8185-8193.
14. M. R. Hoffmann, S. T. Martin, W. Choi and D. W. Bahnemann, *Chem. Rev.*, 1995, **95**, 69-96.
15. Y. Kuwahara and H. Yamashita, *J. Mater. Chem.*, 2011, **21**, 2407-2416.
16. L. Luo, Y. Yang, M. Xiao, L. Bian, B. Yuan, Y. Liu, F. Jiang and X. Pan, *Chem. Eng. J.*, 2015, **262**, 1275-1283.
17. T. Torimoto, S. Ito, S. Kuwabata and H. Yoneyama, *Environ. Sci. Technol.*, 1996, **30**, 1275-1281.
18. D. Liu, W. Cui, J. Lin, Y. Xue, Y. Huang, J. Li, J. Zhang, Z. Liu and C. Tang, *Catal. Commun.*, 2014, **57**, 9-13.
19. X. Fu, Y. Hu, Y. Yang, W. Liu and S. Chen, *J. Hazard. Mater.*, 2013, **244–245**, 102-110.
20. C. Tang, J. Li, Y. Bando, C. Zhi and D. Golberg, *Chemistry – An Asian Journal*, 2010, **5**, 1220-1224.
21. F. Ma, G. Zhao, C. Li, T. Wang, Y. Wu, J. Lv, Y. Zhong and X. Hao, *CrystEngComm*, 2016, **18**, 631-637.
22. Y. Song, H. Xu, C. Wang, J. Chen, J. Yan, Y. Xu, Y. Li, C. Liu, H. Li and Y. Lei, *RSC Adv.*, 2014, **4**, 56853-56862.
23. S. Meng, X. Ye, X. Ning, M. Xie, X. Fu and S. Chen, *Applied Catalysis B: Environmental*, 2016, **182**, 356-368.
24. L. Ma, M. Liu, D. Jing and L. Guo, *J. Mater. Chem. A*, 2015, **3**, 5701-5707.
25. Q. Li, B. Guo, J. Yu, J. Ran, B. Zhang, H. Yan and J. R. Gong, *J. Am. Chem. Soc.*, 2011, **133**, 10878-10884.
26. X. Zhang, G. Lian, S. Zhang, D. Cui and Q. Wang, *CrystEngComm*, 2012, **14**, 4670-4676.
27. J. Li, J. Lin, X. Xu, X. Zhang, Y. Xue, J. Mi, Z. Mo, Y. Fan, L. Hu, X. Yang, J. Zhang, F. Meng, S. Yuan and C. Tang, *Nanotechnology*, 2013, **24**, 155603.
28. M. Shanmugam, R. Jacobs-Gedrim, C. Durcan and B. Yu, *Nanoscale*, 2013, **5**, 11275-11282.

View Article Online
DOI: 10.1039/C6RA20671A

29. A. Kudo and Y. Miseki, *Chem. Soc. Rev.*, 2009, **38**, 253-278.
30. D. Jing and L. Guo, *J. Phys. Chem. B*, 2006, **110**, 11139-11145.
31. Y. Ide, F. Liu, J. Zhang, N. Kawamoto, K. Komaguchi, Y. Bando and D. Golberg, *J. Mater. Chem. A*, 2014, **2**, 4150-4156.

View Article Online
DOI: 10.1039/C6RA20671A

Figure and Captions

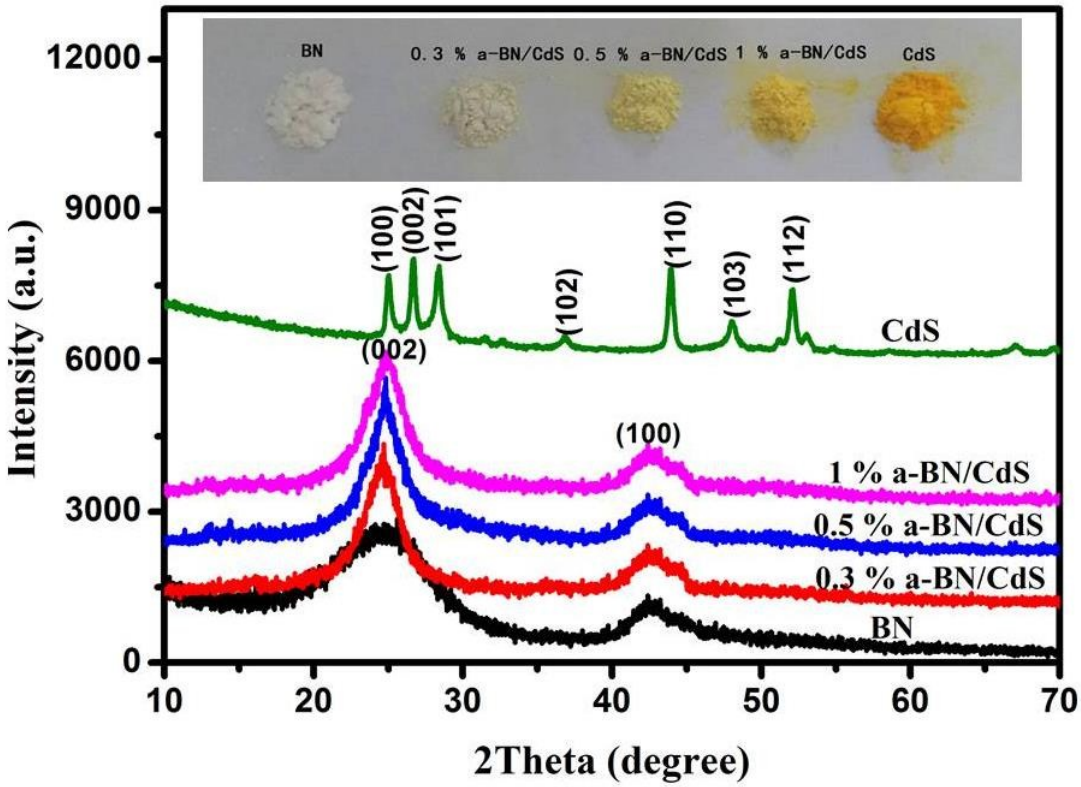

Figure 1. XRD patterns of the prepared porous BN, bulk CdS and a-BN/CdS composites. (Inset: body colors of all of these samples)

View Article Online
DOI: 10.1039/C6RA20671A

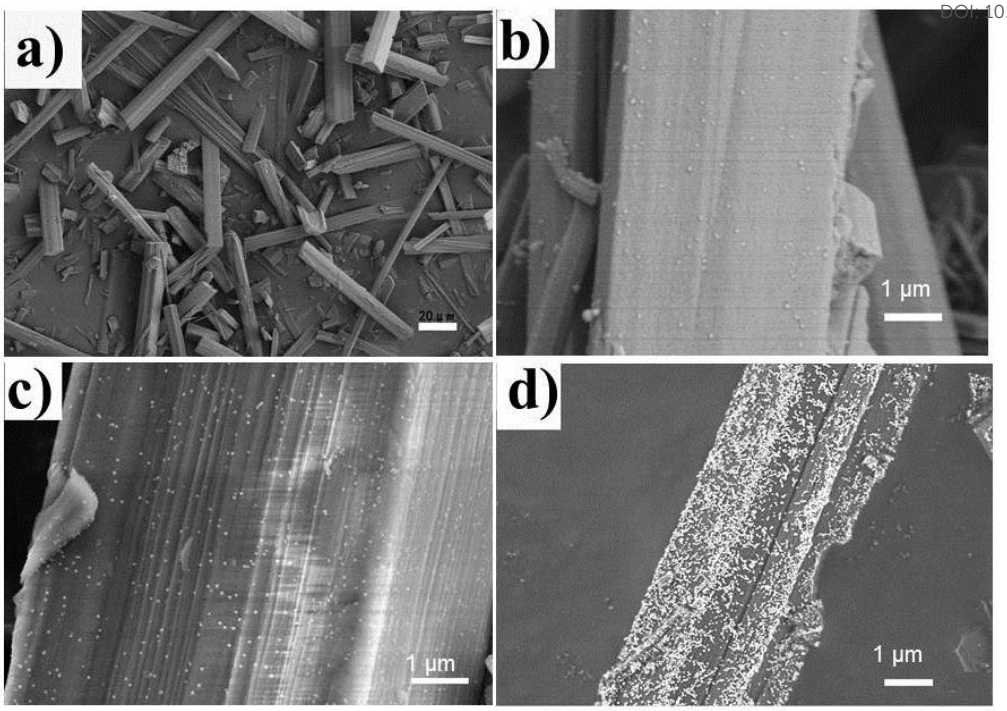

Figure 2. SEM images of: a) pure BN; b) 0.3 % a-BN/CdS; c) 0.5 % a-BN/CdS and d) 1 % a-BN/CdS.

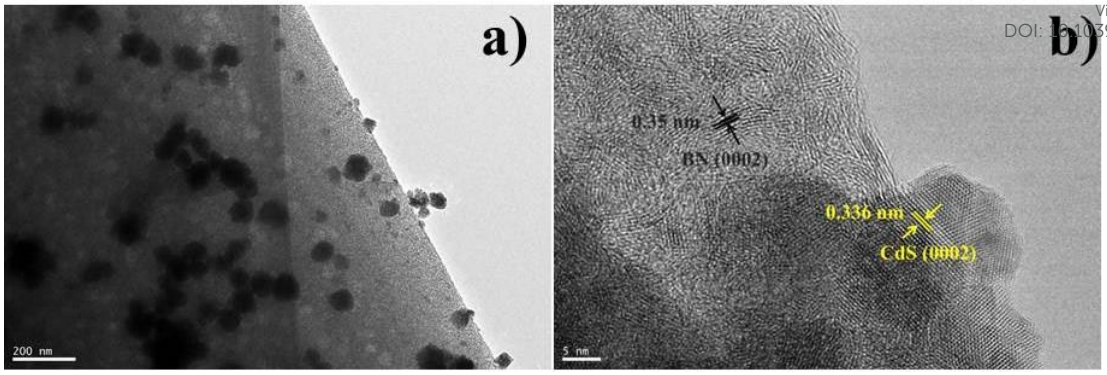

Figure 3. a) TEM image of 0.5 % a-BN/CdS; b) HRTEM image of 0.5 % a-BN/CdS

View Article Online
DOI: 10.1039/C6RA20671A

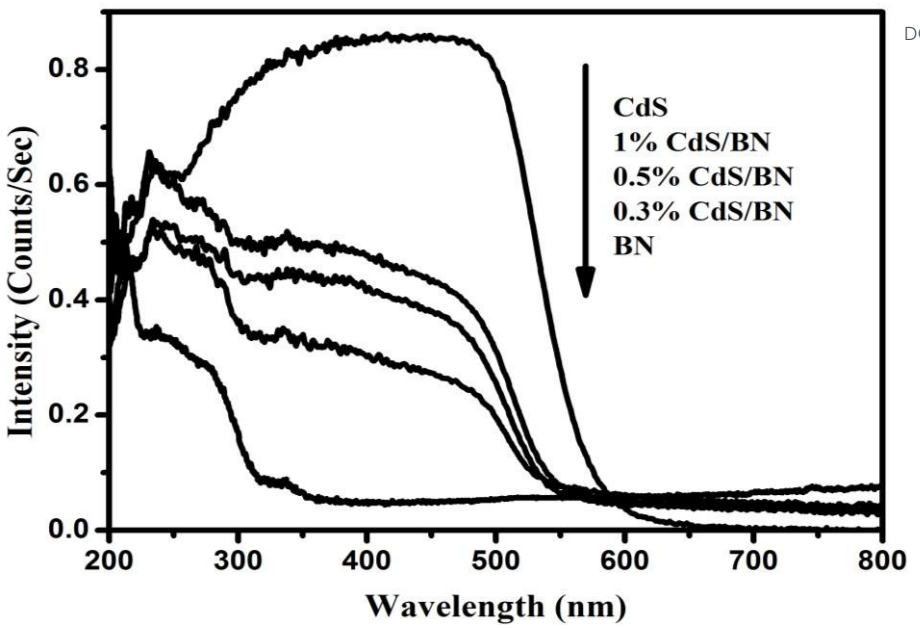

Figure 4. UV-vis diffuse reflectance spectra of pure BN, pure CdS and their composites

View Article Online
DOI: 10.1039/C6RA20671A

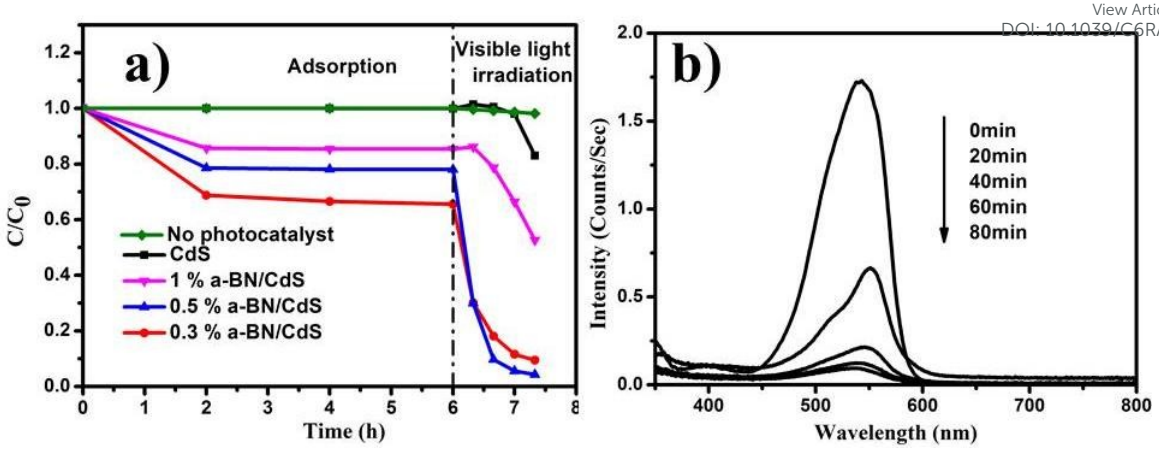

Figure 5. a) Adsorption and photocatalytic degradation processes of RhB on different samples under visible light irradiation; b) UV-vis spectral changes of RhB as a function of irradiation time over 0.5 % a-BN/CdS.

View Article Online
DOI: 10.1039/C6RA20671A

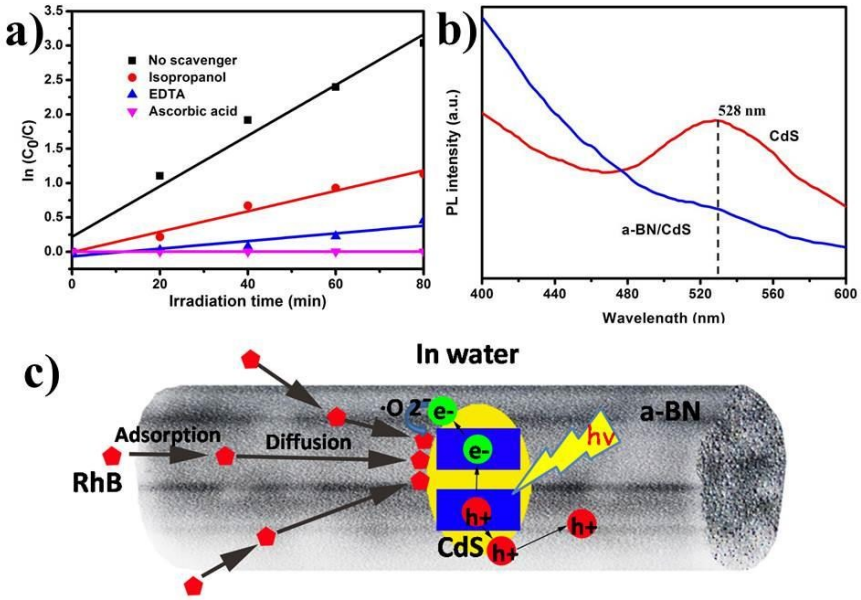

Figure 6. a) Photocatalytic degradation of RhB with 0.5 % a-BN/CdS in the various scavengers under visible light irradiation; b) PL spectra of bulk CdS and 0.5 % a-BN/CdS sample; c) Mechanism of adsorption-photocatalytic synergistic process on RhB under visible light irradiation.

View Article Online
DOI: 10.1039/C6RA20671A

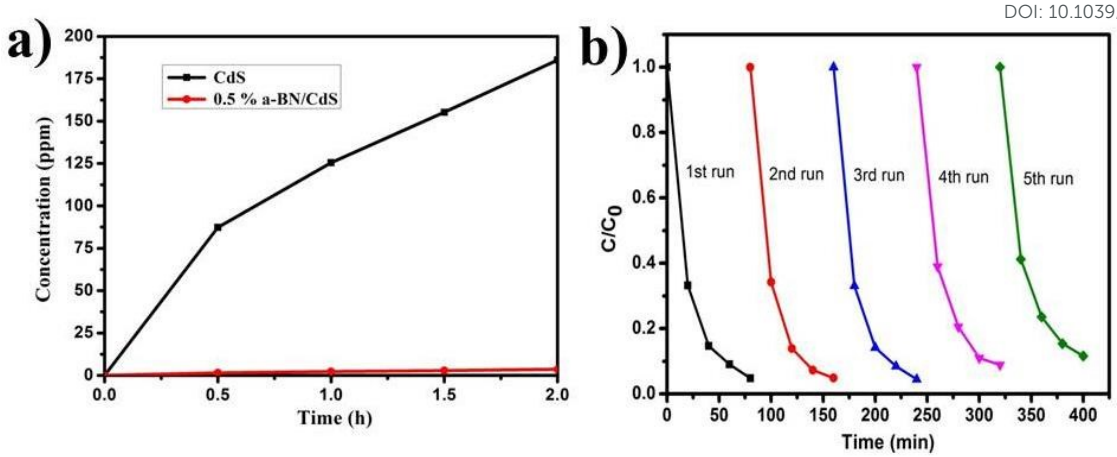

Figure 7. a) The concentration change of Cd^{2+} during the photocatalytic process for bulk CdS and 0.5 % a-BN/CdS by ICP; b) Cycling runs for the photocatalytic degradation of RhB in the presence of 0.5 % a-BN/CdS.

View Article Online
DOI: 10.1039/C6RA20671A

Graphical Abstract

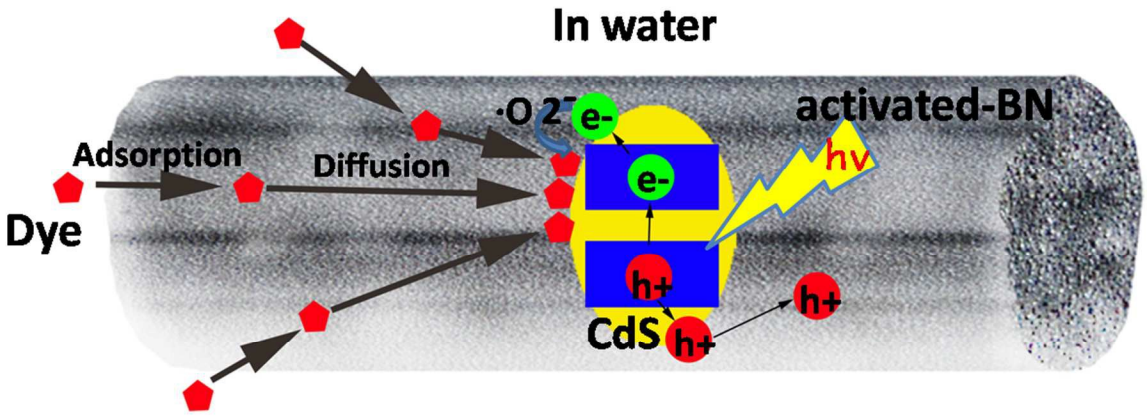

Adsorption-photocatalytic synergistic removal of organic pollutants based on porous BN coupled with a small amount of CdS